A Fully Integrated Arduino-Based System for the Application of Stretching Stimuli to Living Cells and Their Time-Lapse Observation: A Do-It-Yourself Biology Approach

GREGORIO RAGAZZINI,[1,2] JESSICA GUERZONI,[1] ANDREA MESCOLA [ORCID],[2]
DOMENICO DI ROSA,[3] LORENZO CORSI,[3,4]
and ANDREA ALESSANDRINI[1,2,4]

[1]Department of Physics, Informatics and Mathematics, University of Modena and Reggio Emilia, Via Campi 213/A,
41125 Modena, Italy; [2]CNR-Nanoscience Institute-S3, Via Campi 213/A, 41125 Modena, Italy; [3]Department of Life Sciences,
University of Modena and Reggio Emilia, Via G. Campi 287, 41125 Modena, Italy; and [4]INBB (Istituto Nazionale di
Biostrutture e Biosistemi), Viale Medaglie d'Oro 305, 00136 Roma, Italy

Associate Editor Ender A Finol oversaw the review of this article.

Abstract—Mechanobiology has nowadays acquired the status of a topic of fundamental importance in a degree in Biological Sciences. It is inherently a multidisciplinary topic where biology, physics and engineering competences are required. A course in mechanobiology should include lab experiences where students can appreciate how mechanical stimuli from outside affect living cell behaviour. Here we describe all the steps to build a cell stretcher inside an on-stage cell incubator. This device allows exposing living cells to a periodic mechanical stimulus similar to what happens in physiological conditions such as, for example, in the vascular system or in the lungs. The reaction of the cells to the periodic mechanical stretching represents a prototype of a mechanobiological signal integrated by living cells. We also provide the theoretical and experimental aspects related to the calibration of the stretcher apparatus at a level accessible to researchers not used to dealing with topics like continuum mechanics and analysis of deformations. We tested our device by stretching cells of two different lines, U87-MG and Balb-3T3 cells, and we analysed and discussed the effect of the periodic stimulus on both cell reorientation and migration. We also discuss the basic aspects related to the quantitative analysis of the reorientation process and of cell migration. We think that the device we propose can be easily reproduced at low-cost within a project-oriented course in the fields of biology, biotechnology and medical engineering.

Address correspondence to Andrea Alessandrini, Department of Physics, Informatics and Mathematics, University of Modena and Reggio Emilia, Via Campi 213/A, 41125 Modena, Italy. Electronic mail: andrea.alessandrini@unimore.it

INTRODUCTION

It has been largely demonstrated that living cells are affected by mechanical stimuli in a similar way to chemical ones.[1–5] Processes that can be modulated by mechanical cues include differentiation, migration and adhesion and living cells in their physiological environments are continuously exposed to stretching or compressing deformations. These situations include both the case of uniaxial stretching, such as for cells of the skeletal-muscle tissues or cells in the walls of vessels exposed to a periodic stretching given by the blood pressure oscillations, and of isotropic stretching, as in the case of hollow structures such as the heart or lungs. Stretching a cell could affect in different ways its behaviour. For example, stretch-activated ion channels such as piezo-channels[6] could be induced to activate, leading to a change of the flux across the membrane of Ca^{2+} ions, generating in this way a cascade of biochemical processes. At the same time, every deformation of the substrate on which cells are growing acts on the focal adhesion complexes, transmitting the mechanical signal to the cytoskeleton inside the cell.[7–9] Given the mainly dynamic nature of the cell cytoskeleton, a stretching acting on the sticking points of the cells to the substrate, could interfere with the polymerization and depolymerisation processes of its elementary units. To shed light on the role of mechanical stimulation on the cell activity, devices that are able to apply well defined deformations to the

substrate have been developed.[3,10] If cells sufficiently adhere to the underlying substrate, without sliding, a strain of the substrate can be transmitted to their internal structures. Typically, these devices exploit polymer-based compounds on which cells can adhere, proliferate and migrate. Among synthetic polymers, polydimethylsiloxane (PDMS) is largely used as substrate for living cells due to its good biocompatibility and the possibility to tune its rigidity by varying the amount of the crosslinking agent. It should be emphasized that cell adhesion is ultimately regulated by the presence of cell-adhesive molecules, which, depending on the cell type and on the applications, can be natural (e.g. components of the extracellular matrix ECM such as fibronectin or laminin)[11] or obtained with synthetic approaches.[12] These molecules are generally deposited on the substrate surface in contact with cells and are able to locally modify the chemical-physical properties promoting cell adhesion. The substrates can then be stretched periodically by the use of a transducer system. These devices, even if they cannot recapitulate the very complex scenario occurring *in vivo*, can provide very useful information on the biological effects of mechanical deformations of the cells, better approaching specific physiological situations. Indeed, the physiological environment of several cells includes periodic mechanical stimuli, but cells that physiologically reside in regions without mechanical signals also share the same type of reactions when exposed to periodic stretching. This behaviour appears so as a common aspect of the molecular machinery constituting the parts of the cells in mechanical contact with the external environment. It has been demonstrated that cyclic stretching can lead to alterations of the gene expression profile of cells. This phenomenon typically concerns the proteins of the cytoskeleton or associated with it and the proteins of the extracellular matrix.[13–15] One of the effects of periodic stretching on cells that has been deeply investigated is their reorientation relative to the stretching direction in order to maintain a tensional homeostasis.[16–22] There is large evidence that cells with a bipolar shape such as fibroblasts tend to reorganize their orientation almost perpendicularly to the direction of periodic stretching as a consequence of the development of an oriented structure of stress fibers. Studying the details of this effect can largely help in understanding the mechanobiology of the cell/substrate interaction.

The development of mechanical stretching devices represents a sort of interdisciplinary enterprise in which mechanical and medical engineers, together with physicist, biologists and chemists are involved. Several home-developed devices have been described in the literature.[23–32] Commercial devices are also available, such as for example FlexCell (http://www.flexcellint.c om)[33] or STREX (www.strexcell.com) but, in many cases, they have limitations in providing *ad-hoc* stimuli researchers might be interested to test (for example specific periodic signals different from the usual simple sinusoidal, triangular or square patterns).[34] Moreover, they are typically costly to purchase and many laboratories, especially the ones dedicated to educational training, might find it difficult to buy one of them. Moreover, it would also be very interesting to study the kinetics of orientation at high time resolution to understand how a cell responds to a mechanical stimulus transmitted by the environment and what are the main determinants of the phenomenon. For example, the characterization of the relaxation time of the cell orientation process as a function of the applied frequency could be compared with the output of different models that have been developed to describe the overall phenomenon.[35–37] In this case, it would be useful to have a stretcher device integrated with a cell incubator. This result could be pursued both by constructing cell stretcher devices with optical access compatible with an optical microscope[38] and then exploiting an enclosure to maintain all the microscope in the best conditions for cell survival (presence of a CO_2 environment, 37°C and high relative humidity) or by integrating the stretcher device inside an on-stage cell incubator. Only a few devices of the latter type are commercially available and they are typically expensive.

The purpose of this work is twofold and consists, on the one hand, in providing a guide on which to build a project-based course for undergraduate students with the aim of building a cell stretcher device and, on the other, to present some examples of investigations that students could perform with the developed device to get in touch with cutting-edge experiments in the field of mechanobiology. Mechanobiology has in fact developed into a well-established research field that should now be part of undergraduate curricula for biologists, biotechnologists and biomedical engineers. The team of instructors for the project should include both researchers working in laboratories focused on cell biology experiments, where an optical microscope with basic phase imaging systems is typically present, and researchers working in labs more familiar with engineering approaches, where skills such as CAD (Computer Aided Design) knowledge, programming, CNC (Computer Numerical Control) milling techniques and basic electronics are typically present and where there is also the possibility of exploiting a mechanical workshop. The best context for this activity would therefore be a Faculty of Biomedical Engineering. The project presented also includes some ideas on the construction of a motorized stage for optical microscopy (a device available on the market but

usually quite expensive and not included in basic optical microscopes), but, if a large statistical analysis relating to the dynamic behavior of the cell population is not required, this part can be skipped. Before starting the construction of the device the students should attend a short module with some basic concepts of continuum mechanics. These concepts will be exploited for the characterization of the substrate deformations and their quantification. A module where the basic aspects of cell biology, especially the cytoskeleton structure and its functions, are studied is a prerequisite to understand how a mechanical stimulus could be transduced into a biochemical one and, consequently, how the cell could reorient (or reorganize) themselves. Another important module that students should participate in is related to the acquisition of programming skills (C + +, Python and Labview languages for example) in order to interface an instrument with a PC and to design a software to control the device. A short introduction to use of low cost microprocessors such as Arduino is also required. The uniaxial stretching device that we present can be exploited with cell populations growing on a PDMS support while observing how the cells are affected by the mechanical cue with time-lapse optical microscopy imaging. In fact, the stretching device is built inside an on-stage cell incubator.[39] All the different modules are controlled by the Arduino microprocessor and the movements are driven by stepper motors. For the apparatus controlling the cell culturing conditions such as the feedback mechanisms for controlling the temperature and CO_2 concentration, we refer to our previous work.[39] As a proof-of-concept, we will investigate the effect of the periodic stretching stimulus on cell reorientation and migration processes. In the Supporting Material section, we present a brief overview of the different working principles of the stretching devices that have been presented in the literature and a short introduction to mechanobiology as far as mechanical stretching cues are involved. With the low cost device that we present, many educational labs can start proposing tutorial activities on the effects of mechanical cues on the behaviour of living cells.

MATERIALS AND METHODS

Fabrication of the Stretching Device

The stretching device is installed inside an on-stage cell incubator based on a work we recently published.[39] The case is made by a PMMA base and an aluminium wall. The overall scheme of the stretching chamber is shown in Fig. 1. The heating system is composed by thick film resistors mounted on the external wall of two

water reservoirs positioned inside the chamber, as shown in Fig. 1a, and by an ITO (indium-tin-oxide) window positioned on the top cover of the chamber. The window is endowed with two silver-painted lines that assure electrical connection with an external circuit.[39] The heated ITO window provides optical accessibility for time-lapse imaging while avoiding water condensation. The temperature inside the chamber is measured by a DHT22 sensor and is controlled by an Arduino driven circuit exploiting the PID routines already available for this microprocessor. The sensor is positioned inside the chamber very close to the region where the cells are seeded. The position of the cell culture PDMS support is symmetric with respect to the heating apparatus and we can assume the absence of temperature gradients in the incubator chamber in the region close to the cells. The same sensor measures also the relative humidity inside the chamber. The two water reservoir assure the high humidity level inside the incubator with negligible liquid evaporation from the cell medium. For very long imaging sessions (> 24 h), the water reservoirs can be refilled from the outside of the chamber by a tubing system. The CO_2 atmosphere is assured by the same system exploited in our previous work.[39] The mechanical stretching is obtained by a stepper motor controlled by Arduino. The stepper motor produces the rotation of a stainless steel screw with a pitch of 2 mm producing the linear translation of a PVC bar that transmits, via two wires, a symmetrical uniaxial stretching to the cell chamber. All the moving PVC bars of the stretcher device move along two 4 mm diameter aluminium bars using Ball Bearing Linear Bushing typically used for CNC systems. To ensure a completely closed chamber, the region under the PDMS cell substrate was also closed using a glass window. During normal operation of the incubator, this glass window could be subjected to humidity condensation and a consequent deterioration of the image quality. To eventually avoid this problem, a liquid water film can be sandwiched between the bottom of the PDMS chamber and the glass window. This system avoids the formation of a condensation film on the internal face of the window and it is stable without significant evaporation for more than 10 hours. All the drawings of the stretching device are available upon request to the authors.

Cell Culture

The glioblastoma cell line U87MG (ATCC) was grown and maintained in EMEM medium supplemented with 10% fetal bovine serum (FBS), 100 g/mL streptomycin, 100 U/mL penicillin and 1% non-essential amino acids (Euroclone Spa, Milan, Italy)
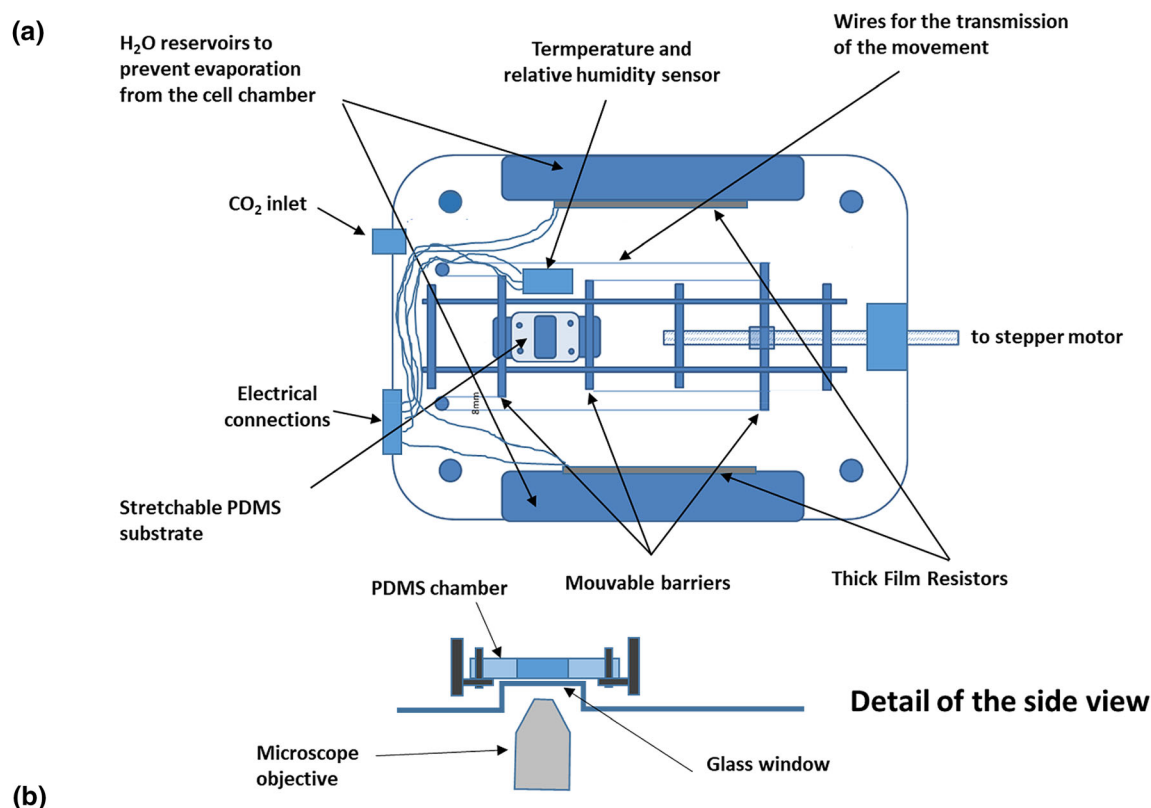
FIGURE 1. (a) scheme of the cell stretcher apparatus. The different parts are highlighted together with the elements used to obtain the controlled environment for the temperature, humidity and CO_2 concentration. (b) top view picture of the stretcher. (c) image of the stretcher mounted on the motorized stage of the inverted optical microscope.

inside a humidified incubator at 37 °C and 5% CO_2. Balb/3T3 clone A 31-1-1 cells (IZSBS, Brescia. Italy) were cultured and maintained in DMEM medium supplemented with 10% FBS and 100 g/mL streptomycin, 100 U/mL penicillin. Sub-confluent cells were then detached using trypsin-EDTA solution (Sigma, Italy) in calcium-free phosphate buffered saline (PBS). For the experiments, U87MG and BALB/3T3 cells were seeded overnight at 5×10^3/cm^2 on PDMS substrates pre-covered with collagen (3%), and fibronectin, respectively, and then, just before the

application of the stretching protocol, the PDMS chamber was transferred from the normal incubator to the on-stage incubator with the stretching system. Cells were then observed in time-lapse during the stretching stimuli. Stress fibers were detected using fluorescent phalloidin and analyzed by fluorescent microscope. Stretched BALB/3T3 cells were fixed with 4% paraformaldehyde at RT, the central region of the PDMS support was cut, and placed on glass coverslips. Cells were then treated with 0,1% Triton X-100 for 20 minutes and blocked with 3% BSA for 30 min. The

cells were then incubated with 7 units/ml Dylight-594-conjugated phalloidin (Thermofisher) for 30 min. in the dark and examined under fluorescent microscope.

Generating the Strain Waveform and Time-Lapse Image Acquisition

There are several pieces of evidence showing how the specific shape of the waveform may have an influence on the effect produced by cyclic stretching on cells (see below). Accordingly, the ability to deliver different waveforms to cells is crucial. In this set-up we can use different waveforms and we also developed a software to be able to provide a periodic deformation resulting from the composition of sinusoidal signals of different frequencies. In this way, a periodic signal of interest can be analysed by a Fourier decomposition process and then reconstructed with the desired fidelity including the required number of harmonic components. See the Supporting Material section for a detailed explanation of the implemented procedure.

Calibration of the Stretching Device

In the Supporting Material all the theoretical aspects on which the calibration of the substrate deformations is based are reported. Here we detail the specific calibration procedure.

To be sure that the stretching of the PDMS substrate responds to the desired stimulus and to calibrate the quantitative substrate stretching we performed a series of experiments with and without cells. We started considering a PDMS substrate without any applied stretch, looking for different features or imperfections of the substrate, such as bubbles encapsulated in the inner part. All this details identify points of reference needed to quantify the amount of deformation reached after gradually increasing the stretching on the substrate. Each time the stretching is increased, a new image is acquired, in order to follow the evolution of the different points identified in the initial frame. In this way we can test if the deformation applied behaves following a homogeneous/linear regime response. The only mechanical boundary condition[40] that we impose to our PDMS substrate is a mechanical clamping as shown in Fig. S4. For the procedure, we concentrated on the central region of the PDMS substrate. Considering that our set-up provides a symmetric stretching, the central position is found by looking for almost static-points during the stretching procedure. Calibration analysis is performed studying the evolution of triads of adjacent points for different regions of the substrate. In this way we can confirm whether the deformations are homogeneous throughout the area, and which are the principal axis along which the deformations act. The amount of strains evaluated along the principal axis are also needed to quantify which is the minimum strain direction in the PDMS substrate (see below). In the following, the complete procedure, is reported for a substrate region.

In Fig. 2, images of the PDMS substrate in unstretched (a) and stretched (b) conditions are reported. In the images we identified five triangles placed at the centre and the four corners of the area. The vertexes of the triangles are identified by features of the substrate. Figure 2c shows an example of the vector analysis. Assuming a common origin in B = B' of the two vectors **BA** and **B'A'**, the deformation vector **AA'** is obtained (see Supporting Material for the complete analysis). For each triangle we can evaluate the associated gradient-deformation matrix $\boldsymbol{F}$ using Eq. [S16]. This matrix contains the transformations involved during the stretching process, in particular, rigid rotation, strain and shear deformation. We can separate rotational contribution from strain and shear by evaluating the right Cauchy-Green deformation tensor, directly ($\boldsymbol{F}^{\mathrm{T}}\boldsymbol{F} = \boldsymbol{C}$) or by polar decomposition of $\boldsymbol{F}$ ($\boldsymbol{F} = \boldsymbol{R}\boldsymbol{U}$) and evaluating the product $\boldsymbol{U}^{T}\boldsymbol{U} = \boldsymbol{C}$. By choosing the polar decomposition we have the possibility to verify if rotational contributions are negligible during deformation. Experimental results obtained from deformation analysis of the five triangles confirm that rigid rotations are negligible. In fact, we obtain $\theta_{\mathrm{Rotation}} = (3.02 \pm 2.87)°$. This evidence confirm that we are deforming the PDMS substrate along two perpendicular directions without introducing any significant rotation. Finally, using the $\boldsymbol{C}$ tensor we can measure the actual strain deformation via the Green-Lagrange strain matrix $\boldsymbol{E}$ ($\boldsymbol{E} = (\boldsymbol{F}^{\mathrm{T}}\boldsymbol{F} - \boldsymbol{I})/2$), which can be also used for large deformation conditions, since $\boldsymbol{F}$ is only a first order strain approximation, useful only for small deformation conditions. We can obtain strain amount along the principal directions using $\boldsymbol{E}$, and compare this results to its first order approximation, provided by $\boldsymbol{F}$ matrix. In fact, we expect from the theory $\boldsymbol{E} \sim \boldsymbol{F}\text{-}1$

From experimental data analysis (see Supporting Material), performed for a well-defined rotation of the stepper motor, we have observed that the strain amount obtained using the Green-Lagrange strain (already diagonalized) is:

$$\boldsymbol{E}(\%) = \begin{pmatrix} \varepsilon_{xx} & 0 \\ 0 & \varepsilon_{yy} \end{pmatrix} = \begin{pmatrix} -3.63 \pm 0.36 & 0 \\ 0 & 10.43 \pm 0.78 \end{pmatrix} \quad (1)$$

Instead, strains obtained using the gradient-deformation matrix $\boldsymbol{F}$ (already diagonalized and subtracting the identity matrix) is:
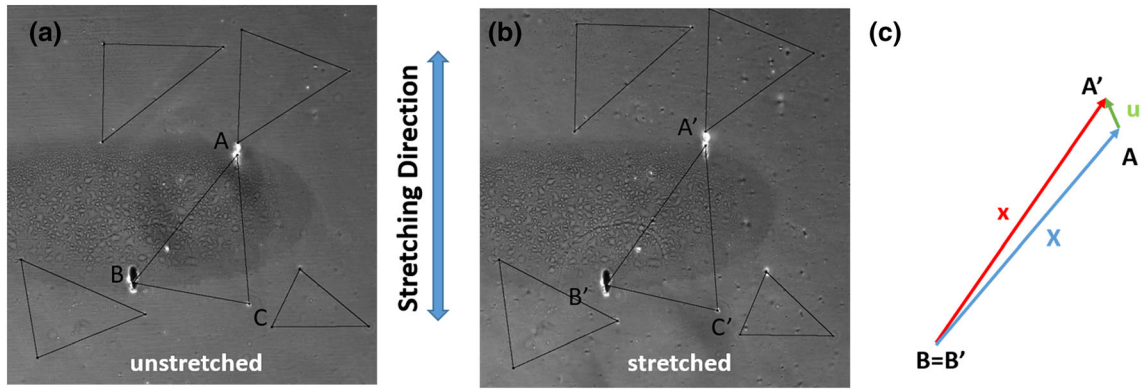
FIGURE 2. (a) PDMS substrate without any applied stretch. The represented triangles were obtained by joining selected features in the substrate; (b) PDMS substrate exposed to stretching via stepper motor rotation. The triangles identified by the same features as in a) were reported; c) Example (enlarged for clarity) of the vector analysis of X = AB (blue) and x = A'B' (red), and the associated u = AA' (green) representing the translational displacement. See Supporting Materials for the complete analysis.

$$\boldsymbol{F} - \boldsymbol{I}(\%) = \begin{pmatrix} F_{xx} - 1 & 0 \\ 0 & F_{yy} - 1 \end{pmatrix}$$
$$= \begin{pmatrix} -3.67 \pm 0.35 & 0 \\ 0 & 9.90 \pm 0.68 \end{pmatrix} \quad (2)$$

The experimental results confirm that $\boldsymbol{F}$ is just a first approximation of the measured strain, which is well described by the matrix $\boldsymbol{E}$. Comparing ε_{xx} with F_{xx}-1 and ε_{yy} with F_{yy}-1, we can observe that the relative error associated to the y axis $\frac{\varepsilon_{yy} - (F_{yy}-1)}{\varepsilon_{yy}} \approx 5.1\%$, the maximum strain direction, is much higher than its counterpart along x axis $\frac{\varepsilon_{xx} - (F_{xx}-1)}{\varepsilon_{xx}} \approx 1.1\%$, the minimum strain direction. This observation is in total agreement with the fact that $\boldsymbol{F}$ is only valid for small deformation. Furthermore, exploiting diagonalization of $\boldsymbol{E}$ we can measure the principal axis strain directions, which are placed at $\theta_{\text{Max-Strain}} \approx 91.48 \pm 3.7°$ and $\theta_{\text{Min-Strain}} \approx 1.48 \pm 3.7°$ for the maximum and minimum strain axis, respectively (using the camera frame as reference). Note that the motor axis producing the stretch is placed at $+90°$, completely in agreement with the measured value of $\theta_{\text{Max-Strain}}$. Also note that the uncertainty associated to $\theta_{\text{Max-Strain}}$ is perfectly comparable to θ_{Rotation} (see Supporting Material for numerical details), the rotation measured by polar decomposition, confirming again that rigid rotation is negligible.

RESULTS AND DISCUSSION

Validation of the Stretching Signal to the Substrate

The signal transmitted to the substrate has been analysed by acquiring images during the stretching cycle at a high frame rate (1 image every 20 ms). The sequence of images was then analysed exploiting the ImageJ plug-in (Align slices in stacks) that allows the alignment of images exploiting a feature present in all images as a reference. A large defect in the substrate has been selected in order to be able to use the same reference for all the images, notwithstanding the focussing problems connected to variations of the z position of the substrate during the stretching process. Once the sequence of images has been aligned, a second feature in the images is selected and the plug-in for the alignment is applied again. The list of the x–y coordinates of the displacements gives variations of the distance between the two selected features during the stretching cycle in the two perpendicular directions. Figure 3 shows two examples for a sinusoidal and a triangular signal. The results related to the validation of the transmission of the stretching signals to cells are reported in the Supporting Material sections. We have verified that the cells are actually stretched following the signal imposed by the substrate.

Cell Reorientation Under the Effect of a Cyclic Stretching Stimulus

In the literature there are many pieces of evidence reporting that cells exposed to a uniaxial cyclic stretching stimulus in a 2D environment reorient themselves in a direction almost perpendicular to the stretching one. If we assume that cells align along the direction of zero strain, we expect to see, after a certain period of continuous cyclic stretching, cells with the major axis of their fitted shape aligned along two mirror directions corresponding to the angle obtained for this specific orientation (see the discussion in the Supporting Material and Eq. S15) (the angle we are considering is evaluated with respect to the main stretching direction). Here we assume that the direc-
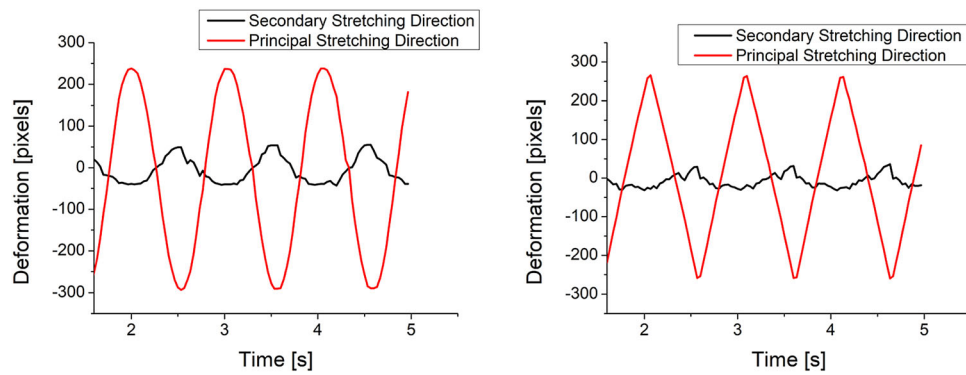
FIGURE 3. analysis of the distance variation between two features in the PDMS substrate for a sinusoidal (a) and a triangular (b) signal. The red line refers to principal stretching direction, black line refers to secondary stretching direction.
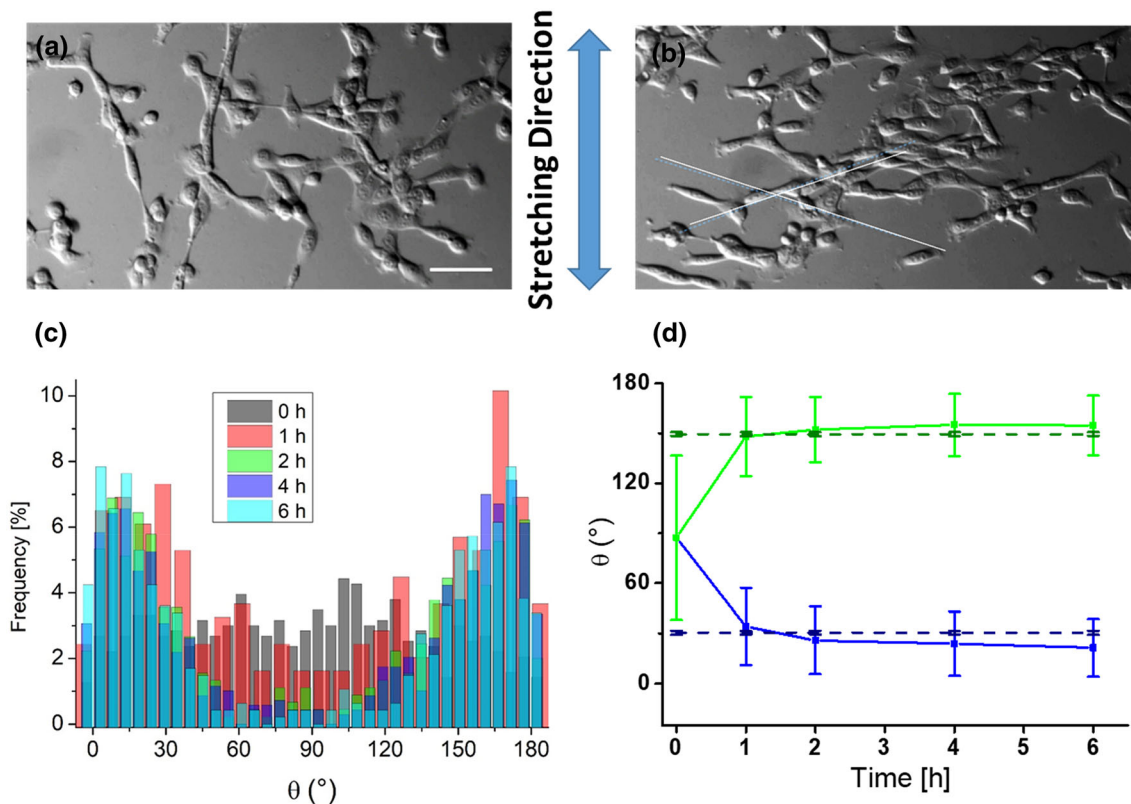

FIGURE 4. Balb-3T3 fibroblast at the beginning of a cyclic stretching experiments (a) and after 6 h of 10% stretching at 1 Hz (b) (bar = 50 μm). The dashed lines are a guide to the eye to highlight the preferred cell orientations. (c) plot of the experimental cell orientation distribution at the beginning of the experiment and after 1, 2, 4 and 6 hours. The distribution of the direction at the beginning of the experiments is given by the grey rectangles. In this specific case, the cell orientation is evaluated in the central position of the sinusoidal cycle; (d) kinetics of mean cell orientation during 6 hours of cyclic stretching. The two horizontal dashed-lines represent the theoretical values for the case of zero strain as obtained from Equation S15.

tion of the cell major axis corresponds to the average direction of the stress fibers in the cell (see below). Accordingly, as shown in the scheme of Fig. S7, the ImageJ software was used to determine the average direction of the major axis of about 100 cells every 2 h of stretching. Figure 4 shows representative images of Balb-3T3 fibroblast cells at the beginning of a stretching experiment (4a) and after 6 hours of cyclic stretching with a sinusoidal signal of 1 Hz and maximum deformation of 10% (4b). Figure 4c shows the distributions of the orientation angles at the different times. In order to have quantitative data about the angular distribution we determined the orientational order parameter $S = \langle \cos 2K \rangle$ where K is the angle

formed by each cell with respect to the average cell direction (the chosen cell director). Accordingly, $S = 0$ means an isotropic distribution of directions, $S = 1$ means perfect order along the director and $S = -1$ means perfect order in the direction perpendicular to the director. The data are reported in Table 1. Figure 4d shows the average cell direction as a function of stretching time. The angles corresponding to the zero strain direction are also reported in Fig. 4d by the two horizontal dashed lines. It is to be stressed that the most probable reorientation process that we observed is represented by cells losing their orientation, becoming almost circular and then extending their body (and stress fibers) along the specific direction of almost zero strain (see below for a detailed analysis) and not a slow rotation of flattened cells.

Whereas at the beginning of the experiment the angle of the major axis of the ellipse used to fit the cell shapes has a uniform distribution (the reference 0° direction is perpendicular to the main stretching direction), after just two hours the direction of the ellipse long axis is mainly distributed along two specific mirror directions, at 15.8° and 165.4 ° with respect to the reference direction. Figure S6 shows the orientation of a single Balb-3T3 cell for two positions in the stretching cycle, highlighting the fact that the orientation of the cell is such to keep an almost constant length while the substrate is stretched.

In a different experiment, at the end of 6 hours of continuous cyclic stretching we evaluated the direction of the cell stress fibers by immunofluorescence microscopy after actin staining and we compared the obtained values with the directions calculated using the cell shape analysis. To obtain the average direction of the stress fibers we exploited the Fast Fourier Transform of the images[41] as reported in Fig. 5. The presence of bright radial regions in the FFT of the images (Fig. 5b) is related to the prevalent directions of the

stress fibers (there is a 90° rotation between the reciprocal space of the FFT and the direct space of the fluorescence image). We then used the Oval profile plug-in of ImageJ to extract the radial integration of the grey values at different angles. The radial integrated intensity is then plotted considering the angular range $0 < K < \pi$ and the maxima in the plot were identified. The results we obtained are reported in Table 2 and match quite well with those obtained exploiting the shape of the cells (we have to consider that the absolute angle is affected by an error due to the alignment of the PDMS substrate after the staining process). However, we have to consider that the kinetics of the two reorientation processes, cell shape and stress fibers, could be different.

In the literature, different scenarios have been observed for the cell realignment kinetics. One possibility is given by a two-step process in which cells, upon feeling the substrate cyclic deformation, get round by a sort of stress fiber fluidization process or an induced rupture in the fibers. The second step foresees a new elongation of the cell in a direction almost perpendicular to the stretching direction followed by a slow rotation up to the final direction follows. From the biochemical point of view, the possible damages to the stress fiber during the elongation step produce a reinforcement thanks to the accumulation of Zyxin and the VASP protein.[42,43] In this context it is important to consider that stress fibers have a viscoelastic behaviour[41] and the rate of the imposed deformation could affect the stress fiber behavior. In another scenario, there could be a rotation of the stress fibers without their destruction. In this case, the rotation could be due to the sliding and reorientation of the focal adhesion complexes.[44] The different behaviour could also be a consequence of the different adhesion strength of the cells to the substrate, where a stronger adhesion could favour the second mechanism. In our case, we mainly observed a behaviour consistent with the first scenario. If, for example, we consider the kinetics of the orientation of a single cell (Fig. 6) we realize that single cells can switch very rapidly from one of the two preferred mirror orientations to the other one. This might be the evidence of a rapid fluidization or rupture of stress fibers and then the formation of new fibers in the preferred directions.[45–47] This behaviour implies that the kinetics of reorientation at the level of a cell population can be difficult to be interpreted according to theories that foresee a gradual reorientation of stress fibers. Accordingly, we concentrated on the kinetics of single cells. The behaviour reported in Fig. 6 can be fitted, in the first part of the reorientation process, by an exponential variation The average time constant we obtain for single cells is of 54 ± 16 min (Fig. S9). The time scale that we

TABLE 1. values of the average direction of cells (± s.d.) and the corresponding S parameter at different time points of continuous cyclic stretching

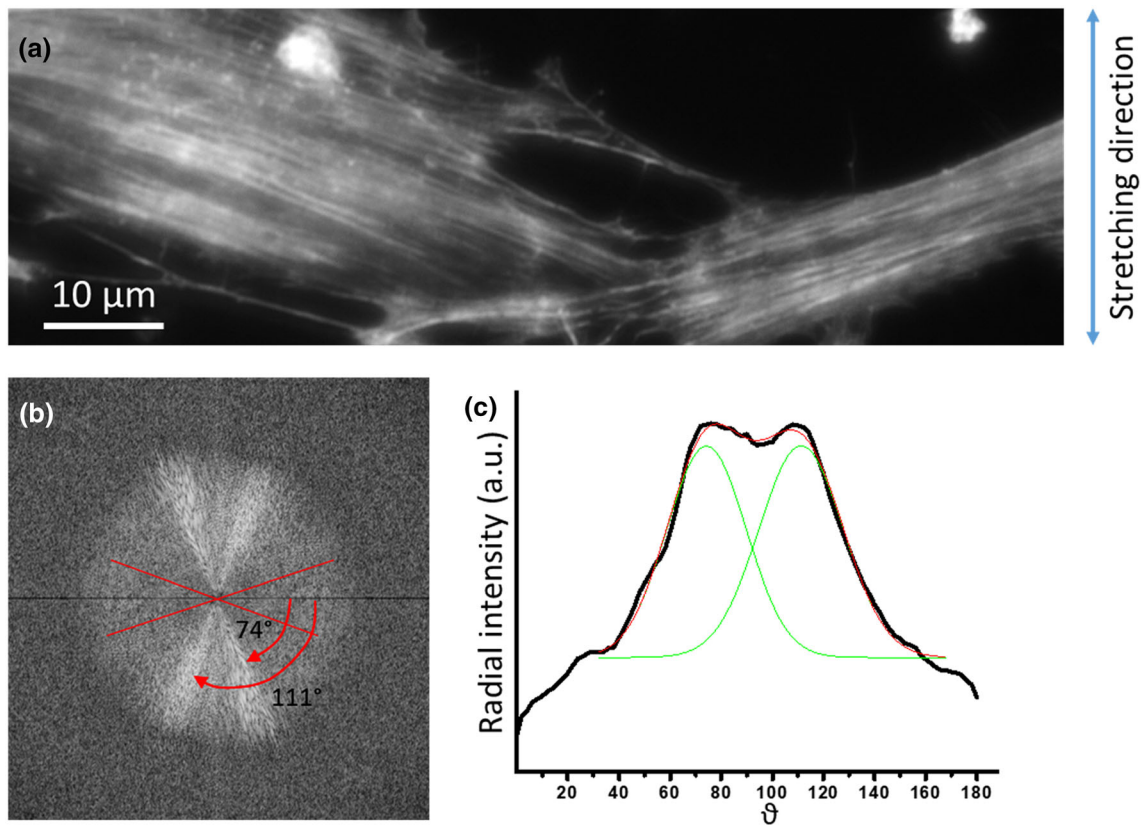| Stretching time	Average direction (director) with respect to the perpendicular to the main stretching direction	S parameter (calculated with respect to the director)
0 h		0.08
1 h	$(34\pm23)°$	0.71 ± 0.30
	$(148\pm23)°$	0.70 ± 0.30
2 h	$(26\pm20)°$	0.79 ± 0.30
	$(152\pm19)°$	0.79 ± 0.20
4 h	$(24\pm19)°$	0.80 ± 0.30
	$(154\pm18)°$	0.81 ± 0.20
6 h	$(21\pm17)°$	0.85 ± 0.30
	$(155\pm17)°$	0.83 ± 0.20

FIGURE 5. (a) Immunofluoresce microscopy image of Balb-3T3 cells at the end of 6 hours of cyclic stretching; b) Fast Fourier Transform (FFT) of (a); (c) radial integration of the grey values of the FFT at different angles

TABLE 2. comparison of the orientations of cell shape and stress fibers

Method	Average direction
6 h Cell shape	$(15\pm14)°$
	$(162\pm16)°$
6 h Stress fibers (based on immunofluorescence)	$(16\pm15)°$
	$(164\pm16)°$

obtained for this process is consistent with what has been reported in the literature for similar experiments.

Cell Migration Under the Effect of a Cyclic Stretching Stimulus

Aside from cell orientation, another aspect of cell behaviour that we have considered, as potentially influenced by cyclic stretch, is 2D migration. We have studied the effect of cyclic stretch on the migration of U87-MG and Balb-3T3 cells. We concentrated on specific aspects of the process of migration such as the direction and the persistence time. The migration direction is measured considering the angle α formed by the line joining the initial and final position of each cell with the direction perpendicular to the stretching direction. In the case of completely isotropic migration, the average value of $|sin\alpha|$ is equal to $2/\pi = 0.64$. A value significantly different from 0.64 can be interpreted as due to a preferential direction of migration. Together with this analysis we have also reported the rose plot of cell migration, providing a qualitative analysis of the migration symmetry, MSD (mean Square Displacement) and autocorrelation of the turning angle.

U87MG cells are characterized by an elevated migration activity[48,49] and their 2D migration is almost independent of the presence of active myosin II, one of the main actors for stress fibers formation and reinforcement.[50] Figure 7a reports the rose plots (left and middle) and the average $|sin(\theta)|$ value (right) for U87MG cells subjected to a 10% sinusoidal stretch at 1 Hz for 7 hours. It appears from both analyses that U87MG cells do not exhibit a preferential direction of migration in the presence of cyclic uniaxial stretching. In fact, control and sinusoidal stretching conditions produce similar behaviors. In Fig. 7b, the comparison between the MSD of unstretched and stretched U87 MG cells is reported. We observed a noticeable difference in the MSD between control and cyclic
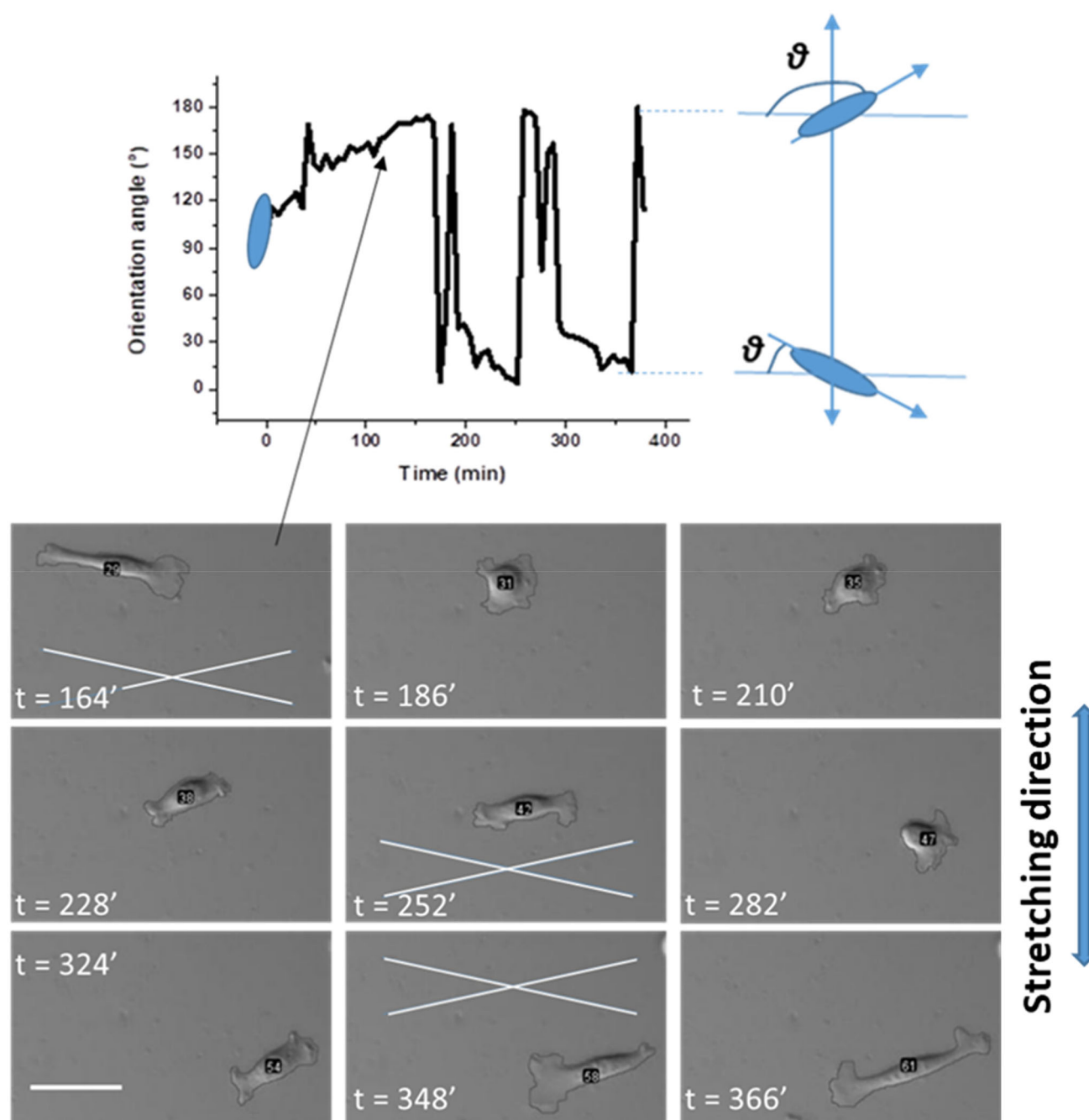
FIGURE 6. Example of the typical reorientation behaviour of a single cell. The angle formed by the long axis of the ellipse fitted to the cell shape is reported for about 400 min of sinusoidal stretching at 1 Hz and 10% maximum stretching. In the bottom, different frames of the corresponding cell are reported. The white lines show the preferred directions of cell orientation. The time of acquisition since the starting of the stretching experiment has been reported for each reported frame (images have been acquired every 6 min). (scale bar = 40 μm)

stretching conditions for time intervals above 200 min, with a higher value for the unstretched condition. The process of cell migration in the absence of directional stimuli can be described as a persistence random walk in which cells, over small time intervals, move in a specific direction but, for long time intervals lose directionality producing a behaviour similar to a random walk. The transition from the short-time behaviour to the long-time one defines the persistence time of the migration, and the distance travelled by cells during this time interval identifies the corresponding persistence length. By fitting the experimental MSD curve with the PRW (Persistence Random Walk) model (Equation S18) we obtain the persistence time
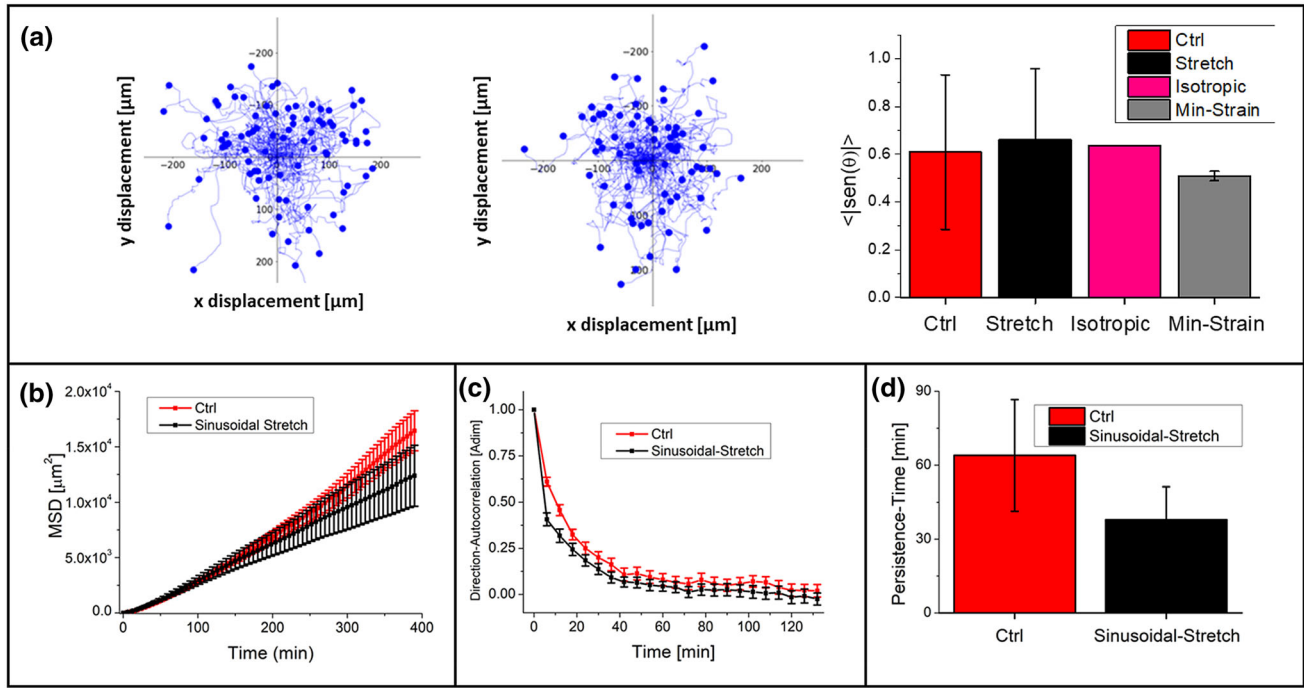
FIGURE 7. analysis of cell migration during the cyclic stretching process for U87MG cells. (a) rose plot for the case of control U87MG cells and U87MG cells exposed to a sinusoidal (1 Hz)stretching protocol (10%) for 6 hours together with the evaluation of the directional migration considering the angle formed by the line connecting the last position of each cell with the initial one for U87Mg cells (the expected value in case of completely isotropic migration and migration along the minimum strain direction are also reported); (b) Mean-Square-Displacement for the migration of U87MG cells on PDMS substrate without any mechanical external stimuli (control condition: red-squares), and on PDMS substrate upon sinusoidal stretching (black squares); (c) autocorrelation analysis of cell migration in the control experiment (red bar) and in the case of the substrate exposed to cyclic stretching (black bar); (d) persistence time calculated according to the Persistent Random Walk (PRW) model for U8MG cells on a PDMS substrate not exposed to cyclic stretching (red-bars) and for cells on a PDMS exposed to cyclic stretching (black-bars)

for the cell migration process (Fig. 7d). In the absence of cyclic stretching, the persistent time P is significantly higher, almost double, compared to cells exposed to periodic stimuli: P = 64±23 min in control condition, P = 38±13 min upon cyclic stretching. An indication of the migration directionality can also be provided by the analysis of the direction autocorrelation[51] (Fig. 7c) as explained in the SM section. Changes in the migration direction provide a sort of indication of the feedback circuits for cell organization, in particular of circuits related to the cytoskeleton organization and to the substrate-cell interactions. From Fig. 7d it appears that, even if no directionality preference is induced by the presence of the directional stretching, the persistence time is reduced by the stretching. Cells in the presence of uniaxial stretching appear to rapidly lose their directional migration. This behaviour could be related to a more difficult stabilization of lamellipodial protrusions and a continuous change of direction as new lamellipodia appear.[52,53] This insight could be confirmed by cell speed distribution comparison obtained by the PRW model fitting on experimental data (Fig. S10). Cell migration both in control condi-

tions and exposed to periodic stretching follow similar normal distribution, and the Gaussian fits of the distributions are almost superimposable. Accordingly, the discrepancy observed in MSD behavior could be ascribed mainly to the variation of the persistence time parameter, supporting the idea that direction changes in cell migration are more relevant than speed modulus.

The results obtained for the migration of Balb-3T3 cells are reported in Fig. 8. The rose plot in Fig. 8a shows a preferential direction of migration for stretched cells, whereas control cells showed a completely isotropic plot. In particular, cells preferentially moved in the direction perpendicular to the stretching direction, as already found for 3T3 cells in the literature.[54] In Fig. 8a we report the final direction of migration, highlighted by the value of $<|\sin(\theta)|>$, after ~7 hours of live cell migration tracking. The experimental result of $<|\sin(\theta)|>$ for cells in control condition is similar to the expected value for isotropic migration, whereas, for periodic stretching condition it is significantly different. We also reported the expected value for migration along the minimum strain direction, previ-
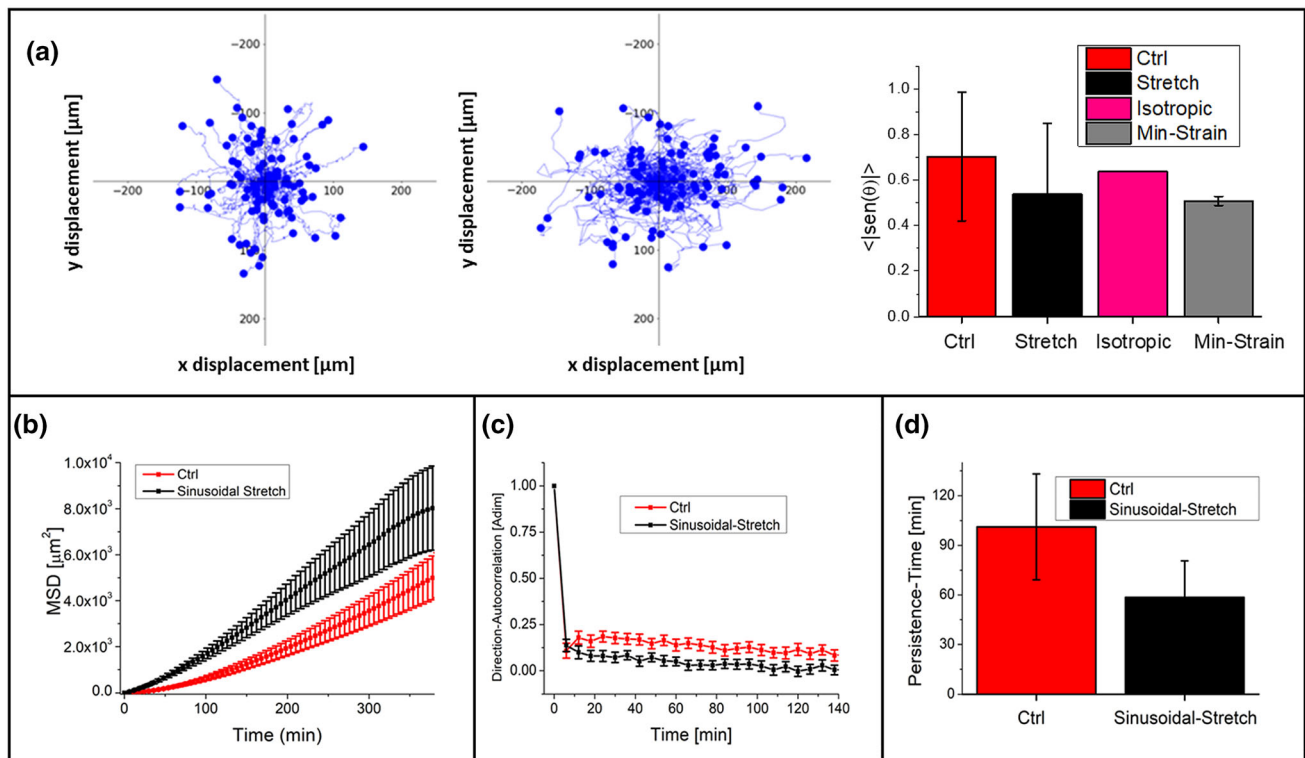
FIGURE 8. analysis of cell migration during the cyclic stretching process for Balb-3t3 cells. (a) rose plot for the case of control cells and cells exposed to a 1 Hz sinusoidal stretching protocol (10%) for 6 hours together with the evaluation of the directional migration considering the angle of the line connecting the last position of each cell with the initial one for Balb-3t3 cells (the expected value in case of completely isotropic migration and migration along the minimum strain direction are also reported); (b) Mean-Square-Displacement graph for cells migration on PDMS substrate without any mechanical external stimuli (control condition: red-squares), and on PDMS substrate upon sinusoidal periodic stretching (black squares); (c) autocorrelation analysis of cell migration in the control experiment (red squares) and in the case of the substrate exposed to cyclic stretching (black squares); (d) persistence time calculated according to the Persistent Random Walk (PRW) model for cells on a PDMS substrate not exposed to cyclic stretching (red-bar) and for cells on a PDMS were exposed to cyclic stretching (black-bar)

ously identified in the stretching calibration section (grey bar). It is interesting to observe that cells exposed to periodic stretching have a value of $|<\sin(\theta)|>$ near to that expected for migration along minimum strain directions. Rose plot comparison could also provide some qualitative cues about the mean area explored by cells. The rose plot comparison does not show any significant discrepancy between control and stretched cells. Figures 8b and 8c show the analysis of the MSD and direction autocorrelation of the cyclically stretched cells compared to the control cells. MSD measured upon periodic stretching is higher than MSD obtained in control condition for the entire period of migration (about 6 hours). Furthermore, the MSD measured at the end of migration analysis for stretched cells is approximately double ($\sim 8 \times 10^3 \ \mu m^2$) compared to the one measured in control condition ($\sim 4 \times 10^3 \ \mu m^2$). This finding provides further supports to previous comments. The direction autocorrelation curves for control and stretching conditions show similar behaviours. However, cells under control con-

dition maintain a slightly higher correlation coefficient over time compared to cells exposed to periodic stretching. This result might appear to conflict with findings obtained for MSD and rose plot. To shed light about this, we analysed the MSD exploiting the PRW model fitting to obtain the persistence time value. Figure 8c shows that the persistence time for cell migration in control conditions is greater than the value obtained for periodic stretching. Persistence time analysis combined with direction autocorrelation comparison suggest that cells in control condition are able to maintain their initial direction for longer time if compared to stretched cells. However, persistence time alone is not able to recapitulate the global MSD behavior. In Fig. S11 the speed parameter distributions obtained by fitting of the PRW model for control condition and for periodic stretching are reported. Both distributions follow a fairly Gaussian trend, but the peak of individual cell speed distribution in control condition is narrow and centred at ~0.3 $\mu m/min$, whereas, for cells exposed to periodic stretching, we

observe a broader peak, centred at a significantly greater speed (~0.6 μm/min). Summarizing, PRW fitting parameters applied to experimental MSD (representing the whole cell population) suggests a strong average cell speed increase when cells are exposed to periodic stretching, together with a persistence time decrease, as also supported by direction autocorrelation finding. However, the speed parameter increment dominates over the time parameter, resulting in a constantly higher MSD for periodic stretching. Furthermore, both direction autocorrelation and persistence time cannot be exploited to highlight the presence, whenever it exists, of a preferential direction of migration.

DISCUSSION

In this work we described how to build from scratch a cell stretcher device exploiting low-cost components. The device is controlled by an Arduino board interfaced with Labview and Python software and is included inside an on-stage cell incubator allowing a time-lapse imaging by optical microscope of how cells react to the mechanical perturbations. All the technical details about the construction of ad-hoc waveforms of the stretching signal have been provided. The theoretical aspects related to the strain calibration of the device have been provided and a detailed step-by-step procedure has been described. We tested the device considering the possible effects of cyclic stretching on the reorientation and migration of cells. Regarding the reorientation effect of cyclic stretching, there is large consensus in the literature about the fact that cells belonging to several lines are able to align themselves in a direction almost perpendicular to the direction of the main deformation stimulus in the case of cyclic stretching. The kinetics and the amount of the average reorientation of a cell population has been found to depend on the amplitude of the stretching stimulus,[20,55] on the frequency[19,56,57] and also on the rate of deformation (the wave shape) for the same value of the overall frequency using non-harmonic stretching protocols.[58–60] Several analytical models have been developed to explain and quantify this phenomenon.[56,61–65] Their validity is evaluated on the basis of the relevant aspects of the phenomenon that they are able to reproduce, such as the dependence upon the frequency and the rate of deformation, the difference between a static stretch and a cyclic stretch, the direction of stress fibers orientation with respect to the substrate strain and the kinetics of cell reorientation. Some of these models are based on methods of statistical mechanics and they rely on the minimization of the potential energy accumulated by the cell cytoskeleton during the stretching process. Accordingly, the orientation of the cells will correspond to the situation in which the stress fibers of the cells are minimally deformed by the substrate. In our study, we found that for cells whose cytoskeletal structure is strongly based on stress fibers, such as Balb-3T3 cells, the periodic stretching produces their realignment in the direction almost perpendicular to the stretching one, whereas, for cells not strongly dependent on stress fibers, like U87 MG cells, the periodic stretching has no relevant effect on their orientation. Considering the specific direction of reorientation, Fig. 4d shows that the average cell orientation at the end of the stretching protocol is slightly different from the theoretical value calculated according to the condition of zero strain. This situation has already been found in the literature and has been differently explained.[66,67] The starting point of the discussion is related to the question of whether the cells perceive the deformation (strain) or the force (stress) to initiate their adaptation process. This aspect has been largely discussed in the mechanobiology context. Pieces of evidence point to a homeostatic process based on the deformation,[68] whereas other experiments pointed to sensitivity of the cells to stress.[69] Cells can also respond in a different way depending on the amount of imposed deformation. We discussed the case in which cells adapt their shape in order to have stress fibers oriented along the direction of zero strain in the Supporting Material section. In the case in which the orientation is controlled by the stress,[35] we have to consider the relations connecting strain and stress of the substrate (plane stress in 2D):

$$\sigma_{xx} = \frac{E}{1 - v^2} \left(\varepsilon_{xx} + v\varepsilon_{yy} \right) \quad (3)$$

$$\sigma_{yy} = \frac{E}{1 - v^2} \left(\varepsilon_{yy} + v\varepsilon_{xx} \right) \quad (4)$$

$$\sigma_{xy} = \frac{E}{1 + v} \varepsilon_{xy} \quad (5)$$

where we have introduced the Young modulus E and the Poisson ratio υ of the material we are using (PDMS). If we consider the ratio σ_{yy}/σ_{xx} we have:

$$\frac{\sigma_{yy}}{\sigma_{xx}} = \frac{\varepsilon_{yy} + v\varepsilon_{xx}}{\varepsilon_{xx} + v\varepsilon_{yy}} = \frac{v - k}{1 - vk} \quad (6)$$

where we used the same symbol $k = -\varepsilon_{yy}/\varepsilon_{xx}$ as in Eq [S14], and the orientation angle will be:

$$\alpha = arctg\sqrt{-\frac{\sigma_{xx}}{\sigma_{yy}}} = arctg\sqrt{\frac{1 - vk}{v - k}} \quad (7)$$

Anyway, as has been reported in Ref 37, the value obtained by this second possibility is not consistent

with the experimental data assuming a value of 0.5 for the Poisson ratio and the experimentally determined value for k. Livne et al. proposed an interesting explanation for this deviation. They considered that the cytoskeleton can be assumed as a 2D elastic system and the direction assumed by the cell is the result of a minimization process of the energy associated with the 2D structure characterized by two different Young Modulus in two perpendicular directions. This theory was able to explain the orientation angle and the kinetics of reorientation exploiting a few variables that remain constant for different stretching conditions.

Considering the effect of cyclic stretching on cell migration, we have to consider that cells can respond to a chemical gradient to establish a specific polarization and migration direction. However, even in the absence of a chemical gradient, cells establish a spontaneous polarization (a sort of symmetry breaking) and start migrating. Migration strategies of cells in this condition reveal important aspects of their survival efficiency.[70] In the literature, a few reports considered the effect of cyclic stretching on migration for fast-crawling cells, such as *Dictyostelium*,[71] that do not have stress fibers, and for cells such as fish keratocytes or different lines that present stress fibers.[72] Since adhesion to a substrate is a requisite for crawling cell migration, it is quite intuitive that a mechanical signal transmitted to the cell cytoskeleton via the underlying substrate could have an effect on the migration speed and direction.[73,74] It has been for example established that, in the case of rat bone marrow stromal cells, cyclic stretching increases their migration capability by an increase of FAK and ERK1/2 action.[75] In other cases, it has been found that cyclic stretching decreases or increases the migration ability of cells that have to heal injuries.[76,77] The different results, regardless of differences in cell lines, could be rationalized considering the time duration of the applied stimulus and a potential adaptation of the cells to cyclic stretching. The presence of a specific polarization induced by the substrate directional stretching can affect the tendency of cells to migrate in a specific direction, without affecting the speed in a specific direction but altering the turning preference of the cells. For example, for *Dictyostelium* cells it has been found that they preferentially migrate along a direction perpendicular to the stretching direction.[78] This effect is the result of a preferential turning of the cell in this direction. Other explanations for an asymmetric directional migration in the presence of periodic stretching could be based on the different distribution of myosin II as a result of local stretching of the actin cytoskeleton.[79] In fact, it has been shown that the non-muscle myosin II interact with actin via a catch-bond,[80] increasing its affinity in regions where the cytoskeleton is more stretched and,

in the case of fast crawling cells, it accumulates on the stretching sides of the cells. Interestingly, in the case of fish keratocytes it has been found that cells preferentially move in the direction of stretching.[72] In this specific case, it is to be considered that cell migration, in normal conditions, occurs in the direction perpendicular to the stress fibers in the cell body. Cyclic stretching can thus align stress fibers and, as a consequence, also migration direction. In our investigation, we found that U87MG cell migration direction is not affected by the cyclic stretching but the persistence time of the migration process, as calculated according to the PRW model is reduced and there is also a discrepancy in MSD behavior (cells in the presence of cyclic stretching explore a smaller area) which can be ascribed mainly to the variation of the persistence time parameter and not to a different cell speed. For Balb 3T3 cells we observed a preferential migration direction in the presence of cyclic stretching. Specifically, migration in the direction perpendicular to the stretching one is favored, cells have a larger MSD and a reduced persistence time. In this case, the larger MSD can be explained by an increased cell speed that overwhelms the persistence time reduction. This analysis shows that other descriptors apart from the directional migration, should be analysed to deeply evaluate the effect of the periodic stretching.

The here proposed project could favour the development of critical thinking and be helpful in mechanobiological studies of the involved students. In particular, the students could learn how an analytical theory about mechanobiology can be developed, considering for example viscoelastic components of the substrate and of the cytoskeleton and the presence of catch-bonds. Indeed, the literature provides different theories about cell reorientation when exposed to cyclic stretch of different amplitude and frequency and then students could plan experiments to establish whether these theories correctly describe the experimental results. Students could also think about the possibility of performing experiments about the differentiation of induced Pluripotent Stems Cells. Indeed, it has been proposed that this type of pluripotent stems cells can be affected by cyclic stretching and the mechanical stimulus could also produce a better maturation of the derived cells.[81–84] Students could also be stimulated to develop critical thinking about the best design of the PDMS culture chamber in order to control the ratio between the deformations in the two perpendicular directions. They could also be encouraged to find different ways to control the stretching of PDMS (for example by the use of voice coils) and they can propose different stretching protocols and different set-ups. They can for example propose a project to develop an isotropic stretcher that could be more rel-

evant to reproduce the behaviour of cells residing in hollow structures.

SUPPLEMENTARY INFORMATION

The online version of this article contains supplementary material available at (https://doi.org/10.1007/s10439-021-02758-3).

REFERENCES

[1]Iskratsch, T., H. Wolfenson, and M. P. Sheetz. Appreciating force and shape — the rise of mechanotransduction in cell biology. *Nat. Rev. Mol. Cell Biol.* 15:825–833, 2014.

[2]Lim, C. T., A. Bershadsky, and M. P. Sheetz. Mechanobiology. *J. R. Soc. Interface* 7:1091–1092, 2010.

[3]Holle, A. W., *et al.* Cell-Extracellular Matrix Mechanobiology: Forceful Tools and Emerging Needs for Basic and Translational Research. *Nano Lett.* 18:1–8, 2018.

[4]Marx, V. May mechanobiology work forcefully for you. *Nat. Methods* 16:1083–1086, 2019.

[5]Jansen, K. A., *et al.* A guide to mechanobiology: Where biology and physics meet. *Biochim. Biophys. Acta Mol. Cell Res.* 1853:3043–3052, 2015.

[6]Coste, B. *et al.* Piezo1 and Piezo2 Are Essential Components of Distinct Mechanically Activated Cation Channels. *Science (80-.).* **330**, 55–60 (2010).

[7]Schwartz, M. A. Integrins and extracellular matrix in mechanotransduction. *Cold Spring Harb. Perspect. Biol.* 2:a005066–a005066, 2010.

[8]Schwarz, U. S., and M. L. Gardel. United we stand – integrating the actin cytoskeleton and cell–matrix adhesions in cellular mechanotransduction. *J. Cell Sci.* 125:3051–3060, 2012.

[9]Kechagia, J. Z., J. Ivaska, and P. Roca-Cusachs. Integrins as biomechanical sensors of the microenvironment. *Nat. Rev. Mol. Cell Biol.* 20:457–473, 2019.

[10]Leung, D. Y. M., S. Glagov, and M. B. Mathews. A new in vitro system for studying cell response to mechanical stimulation. *Exp. Cell Res.* 109:285–298, 1977.

[11]Terranova, V. P., M. Aumailley, L. H. Sultan, G. R. Martin, and H. K. Kleinman. Regulation of cell attachment and cell number by fibronectin and laminin. *J. Cell. Physiol.* 127:473–479, 1986.

[12]Mescola, A., *et al.* Specific neuron placement on gold and silicon nitride-patterned substrates through a two-step functionalization method. *Langmuir* 32:6319–6327, 2016.

[13]Reichenbach, M., K. Reimann, and H. Reuter. Gene expression in response to cyclic mechanical stretch in primary human dermal fibroblasts. *Genomics Data* 2:335–339, 2014.

[14]Lehoux, S., and A. Tedgui. Cellular mechanics and gene expression in blood vessels. *J. Biomech.* 36:631–643, 2003.

[15]Korff, T., K. Aufgebauer, and M. Hecker. Cyclic stretch controls the expression of CD40 in endothelial cells by changing their transforming growth factor–β1 response. *Circulation* 116:2288–2297, 2007.

[16]Hayakawa, K., N. Sato, and T. Obinata. Dynamic Reorientation of Cultured Cells and Stress Fibers under Mechanical Stress from Periodic Stretching. *Exp. Cell Res.* 268:104–114, 2001.

[17]Kurpinski, K., J. Chu, C. Hashi, and S. Li. Anisotropic mechanosensing by mesenchymal stem cells. *Proc. Natl. Acad. Sci. U.S.A.* 103:16095–16100, 2006.

[18]Shirinsky, V. P., *et al.* Mechano-chemical control of human endothelium orientation and size. *J. Cell Biol.* 109:331–339, 1989.

[19]Liu, B., *et al.* Role of cyclic strain frequency in regulating the alignment of vascular smooth muscle cells in vitro. *Biophys. J.* 94:1497–1507, 2008.

[20]Kaunas, R., P. Nguyen, S. Usami, and S. Chien. Cooperative effects of Rho and mechanical stretch on stress fiber organization. *Proc. Natl. Acad. Sci.* 102:15895–15900, 2005.

[21]Brown, R. A., R. Prajapati, D. A. McGrouther, I. V. Yannas, and M. Eastwood. Tensional homeostasis in dermal fibroblasts: mechanical responses to mechanical loading in three-dimensional substrates. *J. Cell. Physiol.* 175:323–332, 1998.

[22]Webster, K. D., W. P. Ng, and D. A. Fletcher. Tensional homeostasis in single fibroblasts. *Biophys. J.* 107:146–155, 2014.

[23]Yost, M. J., *et al.* Design and construction of a uniaxial cell stretcher. *Am. J. Physiol. Circ. Physiol.* 279:H3124–H3130, 2000.

[24]Rana, O. R., *et al.* A simple device to apply equibiaxial strain to cells cultured on flexible membranes. *Am. J. Physiol. Circ. Physiol.* 294:H532–H540, 2008.

[25]Rápalo, G., *et al.* Live cell imaging during mechanical stretch. *J. Vis. Exp.* 2015:1–12, 2015.

[26]Huang, L., P. S. Mathieu, and B. P. Helmke. A stretching device for high-resolution live-cell imaging. *Ann. Biomed. Eng.* 38:1728–1740, 2010.

[27]Schürmann, S., *et al.* The IsoStretcher: an isotropic cell stretch device to study mechanical biosensor pathways in living cells. *Biosens. Bioelectron.* 81:363–372, 2016.

[28]Huang, Y., and N.-T. Nguyen. A polymeric cell stretching device for real-time imaging with optical microscopy. *Biomed. Microdevices* 15:1043–1054, 2013.

[29]Ursekar, C. P., *et al.* Design and construction of an equibiaxial cell stretching system that is improved for biochemical analysis. *PLoS One* 9:e90665, 2014.

[30]Seriani, S., *et al.* The cell-stretcher: a novel device for the mechanical stimulation of cell populations. *Rev. Sci. Instrum.* 87:084301, 2016.

[31]Atcha, H., *et al.* A low-cost mechanical stretching device for uniaxial strain of cells: a platform for pedagogy in mechanobiology. *J. Biomech. Eng.* 140:1–9, 2018.

[32]Boulter, E., Tissot, F. S., Dilly, J., Pisano, S. & Féral, C. C. Cyclic uniaxial mechanical stretching of cells using a LEGO ® parts-based mechanical stretcher system. *J. Cell Sci.* **133**, jcs234666 (2020).

[33]Banes, A. J. Out of academics: education, entrepreneurship and enterprise. *Ann. Biomed. Eng.* 41:1926–1938, 2013.

[34]Lau, J. J., R. M. Wang, and L. D. Black. Development of an arbitrary waveform membrane stretcher for dynamic cell culture. *Ann. Biomed. Eng.* 42:1062–1073, 2014.

[35]De, R., and S. A. Safran. Dynamical theory of active cellular response to external stress. *Phys. Rev. E* 78:031923, 2008.

[36]De, R., A. Zemel, and S. A. Safran. Dynamics of cell orientation. *Nat. Phys.* 3:655–659, 2007.

[37]Livne, A., E. Bouchbinder, and B. Geiger. Cell reorientation under cyclic stretching. *Nat. Commun.* 5:3938, 2014.

[38]Wang, D., *et al.* A stretching device for imaging real-time molecular dynamics of live cells adhering to elastic mem-

branes on inverted microscopes during the entire process of the stretch. *Integr. Biol.* 2:288, 2010.

[39]Ragazzini, G., A. Mescola, L. Corsi, and A. Alessandrini. Fabrication of a low-cost on-stage cell incubator with full automation. *J. Biol. Educ.* 53:165–173, 2019.

[40]Chen, K., et al. Role of boundary conditions in determining cell alignment in response to stretch. *Proc. Natl. Acad. Sci. U.S.A.* 115:986–991, 2018.

[41]Nagayama, K., Y. Kimura, N. Makino, and T. Matsumoto. Strain waveform dependence of stress fiber reorientation in cyclically stretched osteoblastic cells: effects of viscoelastic compression of stress fibers. *Am. J. Physiol. Physiol.* 302:C1469–C1478, 2012.

[42]Smith, M. A., et al. A Zyxin-Mediated Mechanism for Actin Stress Fiber Maintenance and Repair. *Dev. Cell* 19:365–376, 2010.

[43]Smith, M. A., et al. LIM domains target actin regulators Paxillin and Zyxin to sites of stress fiber strain. *PLoS ONE* 8:e69378, 2013.

[44]Deibler, M., J. P. Spatz, and R. Kemkemer. Actin fusion proteins alter the dynamics of mechanically induced cytoskeleton rearrangement. *PLoS One* 6:e22941, 2011.

[45]Trepat, X., et al. Universal physical responses to stretch in the living cell. *Nature* 447:592–595, 2007.

[46]Pirentis, A. P., E. Peruski, A. L. Iordan, and D. Stamenović. A Model for Stress Fiber Realignment Caused by Cytoskeletal Fluidization During Cyclic Stretching. *Cell. Mol. Bioeng.* 4:67–80, 2011.

[47]Krishnan, R., et al. Reinforcement versus Fluidization in Cytoskeletal Mechanoresponsiveness. *PLoS One* 4:e5486, 2009.

[48]Kaphle, P., Y. Li, and L. Yao. The mechanical and pharmacological regulation of glioblastoma cell migration in 3D matrices. *J. Cell. Physiol.* 234:3948–3960, 2019.

[49]Ulrich, T. A., de Juan Pardo, E. M. & Kumar, S. The mechanical rigidity of the extracellular matrix regulates the structure, motility, and proliferation of glioma cells. *Cancer Res.* **69**, 4167–4174 (2009).

[50]Beadle, C., et al. The role of myosin II in glioma invasion of the brain. *Mol. Biol. Cell* 19:3357–3368, 2008.

[51]Gorelik, R., and A. Gautreau. Quantitative and unbiased analysis of directional persistence in cell migration. *Nat. Protoc.* 9:1931–1943, 2014.

[52]Dang, I., et al. Inhibitory signalling to the Arp2/3 complex steers cell migration. *Nature* 503:281–284, 2013.

[53]Krause, M., and A. Gautreau. Steering cell migration: lamellipodium dynamics and the regulation of directional persistence. *Nat. Rev. Mol. Cell Biol.* 15:577–590, 2014.

[54]Goldyn, A. M., Kaiser, P., Spatz, J. P., Ballestrem, C. & Kemkemer, R. The kinetics of force-induced cell reorganization depend on microtubules and actin. *Cytoskeleton* **67**, NA–NA (2010).

[55]Wille, J. J., C. M. Ambrosi, and F. C. P. Yin. Comparison of the effects of cyclic stretching and compression on endothelial cell morphological responses. *J. Biomech. Eng.* 126:545–551, 2004.

[56]Hsu, H.-J., C.-F. Lee, and R. Kaunas. A dynamic stochastic model of frequency-dependent stress fiber alignment induced by cyclic stretch. *PLoS ONE* 4:e4853, 2009.

[57]Jungbauer, S., H. Gao, J. P. Spatz, and R. Kemkemer. Two characteristic regimes in frequency-dependent dynamic reorientation of fibroblasts on cyclically stretched substrates. *Biophys. J.* 95:3470–3478, 2008.

[58]Hsu, H.-J., C.-F. Lee, A. Locke, S. Q. Vanderzyl, and R. Kaunas. Stretch-induced stress fiber remodeling and the activations of JNK and ERK depend on mechanical strain rate, but Not FAK. *PLoS ONE* 5:e12470, 2010.

[59]Lee, C.-F., C. Haase, S. Deguchi, and R. Kaunas. Cyclic stretch-induced stress fiber dynamics—dependence on strain rate, Rho-kinase and MLCK. *Biochem. Biophys. Res. Commun.* 401:344–349, 2010.

[60]Tondon, A., H.-J. Hsu, and R. Kaunas. Dependence of cyclic stretch-induced stress fiber reorientation on stretch waveform. *J. Biomech.* 45:728–735, 2012.

[61]Wang, J. H.-C. Substrate Deformation Determines Actin Cytoskeleton Reorganization: A Mathematical Modeling and Experimental Study. *J. Theor. Biol.* 202:33–41, 2000.

[62]Kaunas, R., and H. J. Hsu. A kinematic model of stretch-induced stress fiber turnover and reorientation. *J. Theor. Biol.* 257:320–330, 2009.

[63]Obbink-Huizer, C., et al. Computational model predicts cell orientation in response to a range of mechanical stimuli. *Biomech. Model. Mechanobiol.* 13:227–236, 2014.

[64]Wei, Z., Deshpande, V. S., McMeeking, R. M. & Evans, A. G. Analysis and interpretation of stress fiber organization in cells subject to cyclic stretch. *J. Biomech. Eng.* **130**, (2008).

[65]Xu, G.-K., B. Li, X.-Q. Feng, H. Gao, and A. Tensegrity. Model of cell reorientation on cyclically stretched substrates. *Biophys. J.* 111:1478–1486, 2016.

[66]Yip, A. K., et al. Cellular response to substrate rigidity is governed by either stress or strain. *Biophys. J.* 104:19–29, 2013.

[67]De, R., A. Zemel, and S. A. Safran. Do cells sense stress or strain? Measurement of cellular orientation can provide a clue. *Biophys. J.* 94:L29–L31, 2008.

[68]Saez, A., A. Buguin, P. Silberzan, and B. Ladoux. Is the mechanical activity of epithelial cells controlled by deformations or forces? *Biophys. J.* 89:L52–L54, 2005.

[69]Freyman, T. M., I. V. Yannas, R. Yokoo, and L. J. Gibson. Fibroblast contractile force is independent of the stiffness which resists the contraction. *Exp. Cell Res.* 272:153–162, 2002.

[70]Li, L., S. F. Nørrelykke, and E. C. Cox. Persistent cell motion in the absence of external signals: a search strategy for eukaryotic cells. *PLoS One* 3:e2093, 2008.

[71]Iwadate, Y., and S. Yumura. Cyclic stretch of the substratum using a shape-memory alloy induces directional migration in Dictyostelium cells. *Biotechniques* 47:757–767, 2009.

[72]Okimura, C., and Y. Iwadate. Hybrid mechanosensing system to generate the polarity needed for migration in fish keratocytes. *Cell Adh. Migr.* 10:1–13, 2016.

[73]Giannone, G., et al. Periodic lamellipodial contractions correlate with rearward actin waves. *Cell* 116:431–443, 2004.

[74]Wang, H.-B., Dembo, M., Hanks, S. K. & Wang, Y. -l. Focal adhesion kinase is involved in mechanosensing during fibroblast migration. *Proc. Natl. Acad. Sci. U.S.A.* **98**, 11295–11300 (2001).

[75]Zhang, B., et al. Cyclic mechanical stretching promotes migration but inhibits invasion of rat bone marrow stromal cells. *Stem Cell Res.* 14:155–164, 2015.

[76]Desai, L. P., S. R. White, and C. M. Waters. Cyclic mechanical stretch decreases cell migration by inhibiting phosphatidylinositol 3-kinase- and focal adhesion kinase-mediated JNK1 activation. *J. Biol. Chem.* 285:4511–4519, 2010.

[77]Nagayama, K., Y. Suzuki, and D. Fujiwara. Directional dependence of cyclic stretch-induced cell migration in wound healing process of monolayer cells. *Adv. Biomed. Eng.* 8:163–169, 2019.

[78]Okimura, C., K. Ueda, Y. Sakumura, and Y. Iwadate. Fast-crawling cell types migrate to avoid the direction of periodic substratum stretching. *Cell Adh. Migr.* 10:331–341, 2016.

[79]Iwadate, Y., *et al*. Myosin-II-mediated directional migration of dictyostelium cells in response to cyclic stretching of substratum. *Biophys. J.* 104:748–758, 2013.

[80]Guo, B., and W. H. Guilford. Mechanics of actomyosin bonds in different nucleotide states are tuned to muscle contraction. *Proc. Natl. Acad. Sci. U.S.A.* 103:9844–9849, 2006.

[81]Saha, S., L. Ji, J. J. De Pablo, and S. P. Palecek. TGFβ/activin/nodal pathway in inhibition of human embryonic stem cell differentiation by mechanical strain. *Biophys. J.* 94:4123–4133, 2008.

[82]Gwak, S. J., *et al*. The effect of cyclic strain on embryonic stem cell-derived cardiomyocytes. *Biomaterials* 29:844–856, 2008.

[83]Mihic, A., *et al*. The effect of cyclic stretch on maturation and 3D tissue formation of human embryonic stem cell--derived cardiomyocytes. *Biomaterials* 35:2798–2808, 2014.

[84]Lee, W. C. C., T. M. Maul, D. A. Vorp, J. P. Rubin, and K. G. Marra. Effects of uniaxial cyclic strain on adipose-derived stem cell morphology, proliferation, and differentiation. *Biomech. Model. Mechanobiol.* 6:265–273, 2007.

Publisher's Note Springer Nature remains neutral with regard to jurisdictional claims in published maps and institutional affiliations.

BMES BIOMEDICAL ENGINEERING SOCIETY